



**HAL**  
open science

## Solubility of L-Glutamic acid in concentrated Water/Ethanol solutions

Maya Khellaf, Catherine Charcosset, Denis Mangin, Elodie Chabanon

► **To cite this version:**

Maya Khellaf, Catherine Charcosset, Denis Mangin, Elodie Chabanon. Solubility of L-Glutamic acid in concentrated Water/Ethanol solutions. *Journal of Crystal Growth*, 2021, 570, pp.126238. 10.1016/j.jcrysro.2021.126238 . hal-03759848

**HAL Id: hal-03759848**

**<https://hal.science/hal-03759848>**

Submitted on 24 Aug 2022

**HAL** is a multi-disciplinary open access archive for the deposit and dissemination of scientific research documents, whether they are published or not. The documents may come from teaching and research institutions in France or abroad, or from public or private research centers.

L'archive ouverte pluridisciplinaire **HAL**, est destinée au dépôt et à la diffusion de documents scientifiques de niveau recherche, publiés ou non, émanant des établissements d'enseignement et de recherche français ou étrangers, des laboratoires publics ou privés.

1

2                   **Solubility of L-Glutamic acid in**

3                   **concentrated Water/Ethanol solutions**

4

5

6                   **Maya KHELLAF, Catherine CHARCOSSET, Denis MANGIN, Elodie**

7   **CHABANON\***

8

9

10           Univ Lyon, Université Claude Bernard Lyon 1, CNRS, LAGEPP UMR 5007, 43

11                   boulevard du 11 novembre 1918, F-69100, VILLEURBANNE, France

12

13

14

15

16

17

18   \*: Corresponding author

19   ☎: +33 4 72 43 18 52

20   Email: [elodie.chabanon@univ-lyon1.fr](mailto:elodie.chabanon@univ-lyon1.fr)

21        **ABSTRACT**

22        In this work the solubility of the metastable  $\alpha$ -form and the stable  $\beta$ -form of L-Glutamic acid  
23        in pure water and in different water/ethanol mixtures at high concentrations of ethanol is  
24        measured by analytical gravimetric method. The experiments are carried out over a temperature  
25        ranging from 283 to 343K. The experimental results show that the solubility of the stable  $\beta$ -  
26        form is lower than the metastable  $\alpha$ -form regardless of the solvent studied (water or  
27        water/ethanol mixtures). The results also highlight that the solubility of both polymorphs  
28        decreases with the increase of the antisolvent concentration and increases with the temperature  
29        rising. Based on the data obtained, the enthalpy and the entropy of dissolution are estimated  
30        thanks to the empirical Van't Hoff correlation. The solubility data of both polymorphs is then  
31        correlated by Combined Nearly Ideal Binary Solution (CNIBS/Redlich-Kister) equation and  
32        the parameters are determined for the temperature studied.

33

34        **KEYWORDS:**

35        A1. Crystallization, A1. Solubility, B1. L-Glutamic acid, B. Water/Ethanol mixtures.

36

## 37        **1. Introduction**

38        Crystallization is an important unit operation in pharmaceutical industry. It is involved during  
39        the process of intermediates products separation and in the final step of active pharmaceutical  
40        ingredients manufacturing. Therefore, it represents one of the most sensitive steps in order to  
41        reach the desired therapeutic objectives of the final compound. Indeed, properties such as  
42        crystal size distribution (CSD), crystal shape, purity and particularly polymorphism have to be  
43        perfectly controlled [1]. In fact, the crystallization of a single molecule can lead to different  
44        crystalline polymorphs depending on the nature of the crystallization (in the melt state or in  
45        solution) and the operating conditions (supersaturation, temperature, nature of the solvent,  
46        impurities...) [2]. They have the same chemical composition but exhibit different physical,  
47        mechanical and thermal properties such as melting point, density, compressibility, hardness and  
48        crystal morphology, as well as solubility and consequently different dissolution rates [1,3,4].

49        These differences in physical properties can have a significant impact on the stability, the  
50        bioavailability (activity/toxicity), the shape of the active ingredient [5] and also on the filtration  
51        and the tableting processes of pharmaceutical and chemical products. A revealing example of  
52        the lack of control of polymorphism is about the production of the drug Norvir<sup>®</sup>, having  
53        Ritonavir as active ingredient, by Abott laboratory. The industrial production of this compound  
54        was stopped following the unexpected appearance of a more stable form. The crystallization of  
55        the metastable form obtained was difficult using seeding or priming [6].

56        Since the crystallization of a selected polymorph is crucial, it is necessary to have an efficient  
57        and reliable production process for the targeted polymorph [7].

58        The current issue is to develop methods enabling a good control of CSD and polymorphisms.  
59        Nowadays, antisolvent crystallization in stirred reactor is the most implemented technique at  
60        the industrial scale [8]. In spite of the process robustness, micro-mixing heterogeneity can be

61 encountered, affecting the production repeatability, the final product homogeneity [9] or even  
62 the polymorphic phase formed. To limit these problems, reverse antisolvent crystallization is  
63 proposed as an alternative method, i.e. the solvent is selectively removed from a  
64 solvent/antisolvent solution in order to increase the supersaturation and induce the nucleation.  
65 This technique might have some advantages: higher yield, limited phase transition allowing  
66 better control of polymorphism and more uniform supersaturation. But, the knowledge of the  
67 solubility data of polymorphs in the solvent/antisolvent mixtures is essential to the  
68 crystallization process and product quality control. That is the purpose of this study.

69 L-Glutamic acid, one of the main amino acids used in pharmaceutical and food industries [10],  
70 has been chosen as a model compound. This molecule crystallizes under two well-known  
71 monotropic polymorphs: the stable polymorph  $\beta$  and the metastable polymorph  $\alpha$ , wherein the  
72  $\beta$ -form is needle-like in shape and the  $\alpha$ -form is prismatic. The solubility data of both  
73 polymorphs in pure water at different temperatures has already been determined in previous  
74 works [11–13]. Also, some studies reported the solubility data of  $\alpha$ -form and  $\beta$ -form in different  
75 solvent/antisolvent mixtures [10,12,14]. However, the data in water/ethanol mixtures are still  
76 limited and therefore more consistent results are needed, especially at high ethanol  
77 concentration.

78 In the present work, the solubility data of  $\alpha$ -form and  $\beta$ -form of L-Glutamic acid in  
79 water/ethanol solutions are measured by a gravimetric method. The enthalpy and the entropy  
80 of dissolution of both polymorphs are then determined based on regression of the solubility data  
81 thanks to the Van't Hoff equation. Finally, the experimental data in the investigated  
82 water/ethanol mixtures are correlated with the thermodynamic model CNIBS/Redlich-Kister  
83 based on three parameters related to the binary and ternary interactions between the three  
84 species (solute, antisolvent and solvent), which are determined as function of the temperature.

## 86        2. Experimental section

### 87            2.1. Materials

88        The stable  $\beta$  polymorph of L-Glutamic acid, purchased from Sigma Aldrich Co. Ltd (Lot  
89        BCBT9726, purity  $\geq 99.5\%$ ), absolute anhydrous ethanol for analytical grade from Carlo Erba  
90        Reagent S.A.S (chemical purity  $\geq 99.9\%$ ) and ultrapure water (resistivity =  $18.2\text{m}\Omega\cdot\text{cm}$ ) are  
91        used to perform the solubility measurements reported below.

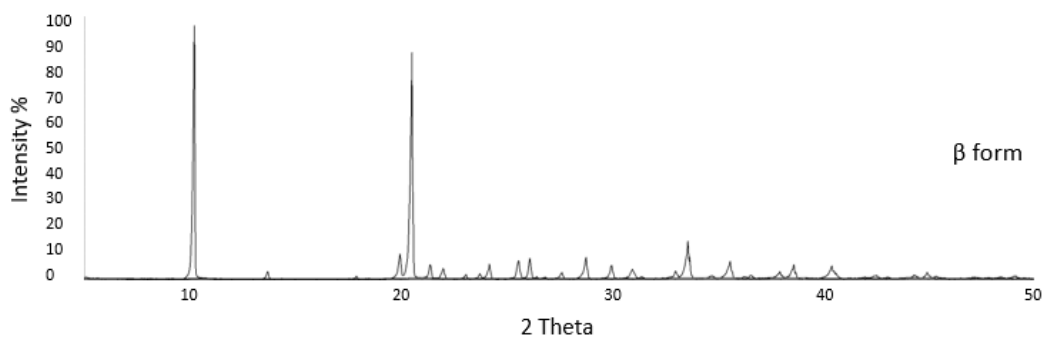
### 92            2.2. Preparation of $\alpha$ L-glutamic acid

93        First of all, a sample of the commercial L-Glutamic acid is analyzed by X-Ray Diffraction  
94        (XRD) in order to confirm the presence of the stable phase  $\beta$  only. The pure  $\alpha$ -form is obtained  
95        following the protocol described by Tahri et al. [11]. For this purpose, an aqueous solution of  
96        L-Glutamic acid (15g/kg of solvent) is rapidly cooled from  $50^\circ\text{C}$  to  $5^\circ\text{C}$  at a rate of  $-1.5^\circ\text{C}/\text{min}$   
97        and under constant stirring. After about 1 h at  $5^\circ\text{C}$ , the nucleation and the growth of the  $\alpha$ -form  
98        occurs and can be observed thanks to a video probe (EZProbe® 12005) immersed in the reactor.  
99        The suspension is then quickly filtered and dried at room temperature. Optical Microscopy  
100        (OM) observations are first carried out to identify the crystals obtained. Then, XRD and  
101        Scanning Electron Microscopy (SEM) analyses are achieved to confirm the presence of the  
102        desired polymorphic form and to observe its morphology, respectively. The XRD patterns are  
103        recorded on a Bruker D8 Advance Diffractometer at room temperature with  $\text{Cu K}\alpha$  radiation of  
104        wavelength  $1.54060\text{\AA}$ , a tube voltage of  $40\text{kV}$  and a tube current of  $40\text{mA}$ . The diffraction  
105        spectra are recorded by a step scanning method at 2 Theta values between  $5^\circ$  and  $50^\circ$  with a  
106        step size of  $0.02^\circ$ . The SEM analyses are carried out with a FEI Quanta 250 FEG microscope.  
107        The crystals are deposited on a flat steel holder before being sputtered with  $20\text{nm}$  of copper  
108        under high vacuum and then observed under an accelerating voltage of  $15\text{KV}$ .

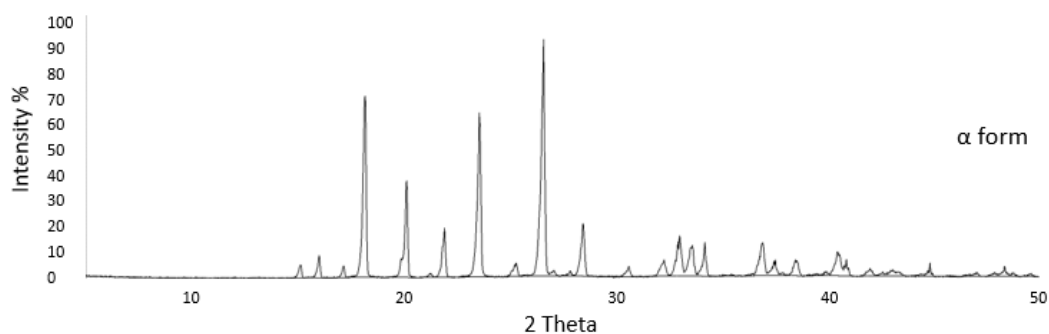
109 Fig. 1. presents the observations obtained by OM and SEM. It is worth noting that, as expected,  
110 the  $\alpha$ - form is prismatic while the  $\beta$ -form is needle-like. Fig. 2. represents the XRD patterns of  
111 both polymorphs. The patterns show the presence of only one polymorph in each case.



112  
113 **Fig. 1.** OM (top) and SEM (bottom) micrographs of the stable  $\beta$ -form (a1, a2) and the  
114 metastable  $\alpha$ -form (b1, b2) of L-Glutamic acid



116



117

118 **Fig. 2.** XRD patterns of the stable  $\beta$  and the metastable  $\alpha$  polymorphs of L-Glutamic acid

119

### 2.3.Apparatus and procedure for the solubility measurement

120 The solubility measurements are, first, performed in pure water and compared with the data

121 available in the literature in order to validate the experimental protocol. Then, solubility of both

122 polymorphs are measured in different water/ethanol solutions with  $x_{EtOH}$  the initial molar

123 fraction of ethanol determined in the absence of L-Glutamic acid and ranging from 0 to 31.9%

124 (0 to 54.5%wt). To achieve that, a slurry of  $\alpha$ -form or  $\beta$ -form is prepared by adding an excess

125 of solute to the solvent mixture in a 100mL stirred double jacketed reactor. The reactor (cf.

126 Fig.3) is equipped with a condenser to avoid any solvent evaporation during the heating phase

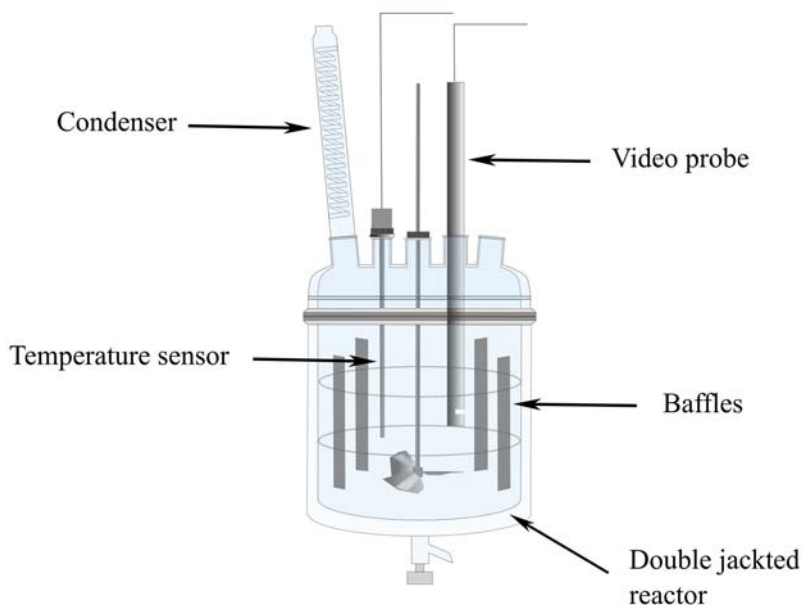
127 and agitated with a 3-blade mixel TT<sup>®</sup> propeller. The temperature is controlled by a bath

128 circulation thermostat (ministat 230, Huber, Germany) equipped with a pt100 sensor and

129 checked by a Platinum resistance thermometer using a multimeter (2700 multimeter, Keithley,

130 US).





131

132

**Fig. 3.** Experimental set-up

133 The composition of the saturated solution is determined by gravimetric method which has  
134 already been reported in several studies to measure the solubility of L-Glutamic acid [10–12].

135 The first step is to determine the time required for the solution to reach the thermodynamic  
136 equilibrium. This has been done at the lowest temperature studied (283K) since the kinetic  
137 should be the lowest at this temperature. An excess of solid is added to the solution and two  
138 samples are collected every 1h, with a 2mL pipette equipped with a filter, and then, placed in  
139 an oven at 358K for 24h. All the samples are weighted before and after drying (at room  
140 temperature), using an analytical balance (XA105 DualRange, Mettler Toledo, Switzerland)  
141 with  $\pm 0.01\text{mg}$  accuracy, and the solubility of L-Glutamic acid is deduced. Based on the results  
142 obtained (cf. Fig.4), the duration of 2h30 for pure water and 2h for water/ethanol mixtures,  
143 whatever the molar fraction of ethanol ( $x_{\text{EtOH}}$ ), are selected to measure the solubility of both  
144 polymorphs between 283K and 343K following the same gravimetric method described above  
145 [11,12,15].

146 Since  $\alpha$  is the metastable form in the whole studied temperature domain, it was important to  
147 ensure that no phase transition towards  $\beta$  form occurred during  $\alpha$  polymorph solubility  
148 measurement [16]. Thus, the suspension was monitored with an *in situ* video probe directly  
149 immersed in the stirred vessel and suspension samples were regularly withdrawn and observed  
150 by OM (optical microscopy). In fact, for temperature above 328K and ethanol molar fraction  
151 under 0.171, it was observed that the phase transition had started at the time of the solubility  
152 measurement. However, the dissolution rate of  $\alpha$ -form is faster than the growth rate of  $\beta$ -form.  
153 As a consequence, although both phases were present in suspension, the solution concentration  
154 remained close to the  $\alpha$ -polymorph solubility [12,17,18]. This is also in agreement with the  
155 Van t'Hoff plot of  $\alpha$ -form solubility (see Fig. 6), which does not show any change in slope in  
156 the whole temperature domain and whatever the solvent mixture composition. Besides, Long  
157 et al. [10] and Tahri et al. [11] have already measured the  $\alpha$  polymorph solubility at  
158 temperatures up to 343K in pure ethanol and pure water respectively. It will be seen below, that  
159 the  $\alpha$ -form solubility in water presented in this work is close to the results reported by Tahri et  
160 al. Finally, it has to be mentioned that a low phase transition was observed for temperature  
161 above 333K and ethanol molar fraction over 0.236 within the experimental time. Indeed, it is  
162 well-known that phase transitions are slowed down when solubility is very low.

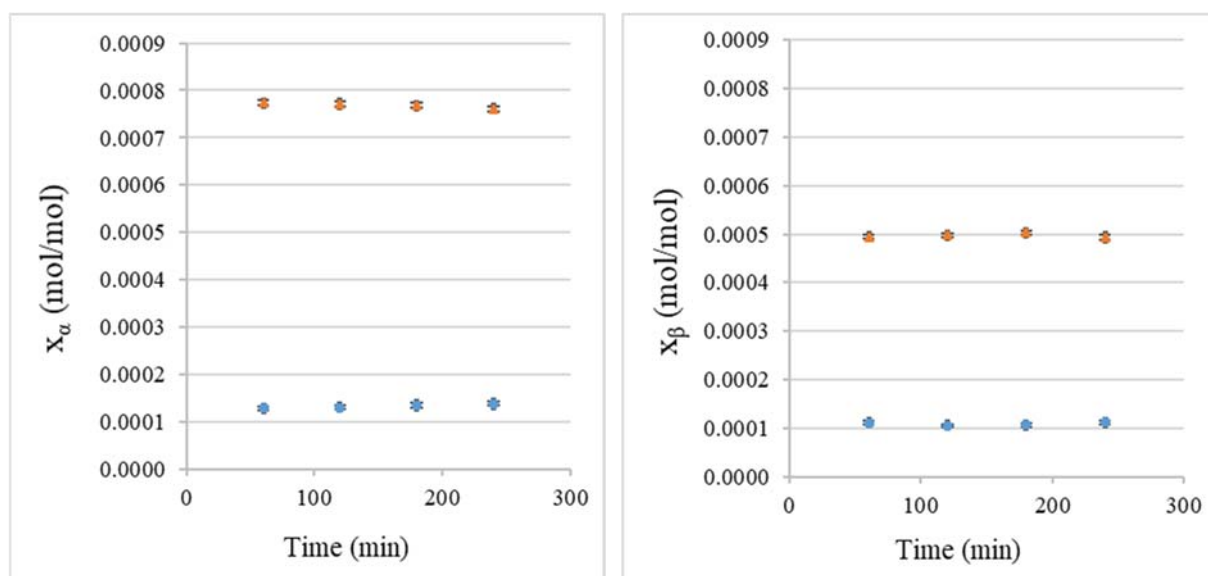
163

164 The molar fraction solubility ( $x_i$ ) of each polymorph of L-Glutamic acid ( $i=\alpha$  or  $\beta$ ) in the  
165 solvent mixtures is calculated as follow:

$$166 \quad x_i = \frac{m_i/M_i}{m_i/M_i + m_w/M_w + m_{EtOH}/M_{EtOH}} \quad (1)$$

167 Where  $m_i$ ,  $m_w$ , and  $m_{EtOH}$  represent the masses (in g) of dissolved L-Glutamic acid), water  
168 and ethanol, respectively and  $M_i$ ,  $M_w$  and  $M_{EtOH}$  are the molecular weights (in g.mol<sup>-1</sup>) of L-  
169 Glutamic acid, water and ethanol, respectively.

170 The error of the solubility measurements is estimated by taking 10 samples at the same  
171 temperature. The standard deviation is then calculated, divided by the square root of the number  
172 of samples and multiplied by 2.262 (which corresponds to a confidence level of 95%). The error  
173 obtained is  $\pm 5.03 \cdot 10^{-6}$ .



174

175 **Fig. 4.** Thermodynamic equilibrium study of  $\alpha$  and  $\beta$ -forms at 283K in ( $\blacktriangle$ ) pure water and  
176 in ( $\bullet$ )  $x_{\text{EtOH}} = 0.236$ .

### 177 3. Result and discussion

#### 178 3.1. Solubility data

179 In this work, the solubility data of both polymorphs of L-Glutamic acid in pure water and in  
180 water/ethanol mixtures are investigated on a temperature range from 283K to 343K. The crystal  
181 shape is checked by OM observation for each measurement.

182 The results obtained are listed in Table 1 and presented in Fig. 5 where  $x_\alpha$  and  $x_\beta$  represent the  
183 molar fraction solubility of  $\alpha$ -form and  $\beta$ -form, respectively, and  $x_{\text{EtOH}}$  denotes the molar  
184 fraction of ethanol in the solvent mixture (without considering the L-Glutamic acid).

185 As it can be seen on Fig. 5, the solubility data reached in pure water in this work are in good  
186 agreement with the data available in the literature [11,12].

187 Table 1 shows that the solubility of both polymorphs increases with increasing the temperature.  
188 Another point is that the  $\alpha$ -form has a higher solubility than the  $\beta$ -form over the entire  
189 temperature range studied, confirming, thus, that  $\beta$ -form is the thermodynamically stable form  
190 and  $\alpha$  the metastable one. However, it can be noticed from Table 1 that the solubility of the  
191 stable  $\beta$ -form and the  $\alpha$ -form are 0.93 and 0.82 respectively at  $T=283$  K and  $x_{\text{EtOH}}=0.319$ ;  
192 Similarly, the solubility of the stable  $\beta$ -form and the  $\alpha$ -form are 1.4 and 1.37 respectively at  
193  $T=293$  K and  $x_{\text{EtOH}}=0.319$ . These solubilities are not in agreement with the respective stability  
194 of  $\alpha$  and  $\beta$  forms. Nevertheless, at such high concentrations of ethanol and low temperatures,  
195 the solubilities of both polymorphs are extremely low and are nearly similar, the difference  
196 between the two values is within the error range of  $\pm 5.03 \cdot 10^{-6}$ .  
197 According to the results obtained, it has to be noted that the solubility of the polymorphs  
198 decreases with the increase of the antisolvent, i.e. the ethanol, concentration.  
199 The relative standard deviation (RSD) of the solubility measurements of  $\alpha$ -form and  $\beta$ -form are  
200 calculated based on the results obtained by the equation (2):

$$201 \quad \text{RSD} = \frac{\sigma_i}{\bar{x}_i} \times 100 \quad \text{with} \quad \sigma_i = \sqrt{\frac{\sum_{i=1}^n (x_i - \bar{x}_i)^2}{n-1}} \quad (2)$$

202 where  $\sigma_i$  is the standard deviation of the solubility measurement (mol/mol) at temperature  $T$ ,  
203  $x_i$  and  $\bar{x}_i$  are respectively the solubility value of the polymorph  $i$  (i.e.  $\alpha$  or  $\beta$ ) and the average  
204 solubility (mol/mol),  $n$  is the number of samples.

205 For instance, the RSD is about 3.07% and 3.05% for 0.236 ethanol molar fraction at 283K for  
206  $\alpha$  and  $\beta$  forms respectively, and 0.7% and 0.89% in pure water at 283K for  $\alpha$  and  $\beta$  forms  
207 respectively. These values are less than 5%, indicating the validity of the solubility  
208 measurements.

209

210 **Table 1**

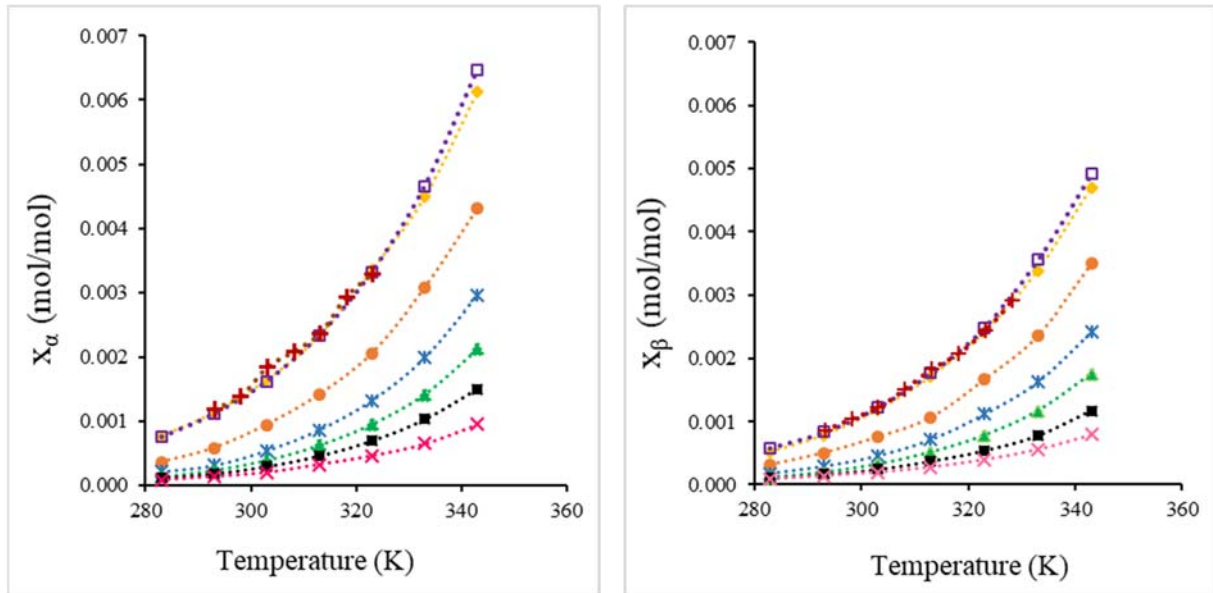
211 Molar fraction solubility of  $\alpha$ -form ( $x_\alpha$ ) and  $\beta$ -form ( $x_\beta$ ) in pure water and in water/ethanol  
 212 mixtures with different molar fractions of ethanol ( $x_{\text{EtOH}}$ ) as a function of temperature T.

213

T (K)	$10^4 \times x_\alpha$	$10^4 \times x_\beta$	T(K)	$10^4 \times x_\alpha$	$10^4 \times x_\beta$	T(K)	$10^4 \times x_\alpha$	$10^4 \times x_\beta$
<b>Pure water</b>			<b><math>x_{\text{EtOH}}=0.051</math></b>			<b><math>x_{\text{EtOH}}=0.116</math></b>		
<b>283</b>	7.69	5.15	<b>283</b>	3.63	3.18	<b>283</b>	2.14	1.76
<b>293</b>	11.40	7.81	<b>293</b>	5.85	5.06	<b>293</b>	3.13	2.88
<b>303</b>	16.45	11.82	<b>303</b>	9.50	7.54	<b>303</b>	5.42	4.53
<b>313</b>	23.33	17.11	<b>313</b>	14.21	10.67	<b>313</b>	8.69	7.12
<b>323</b>	33.51	24.17	<b>323</b>	20.67	16.69	<b>323</b>	13.29	11.16
<b>333</b>	44.90	33.87	<b>333</b>	30.82	23.64	<b>333</b>	19.96	16.27
<b>343</b>	61.30	47.01	<b>343</b>	43.19	34.95	<b>343</b>	29.64	24.17
<b><math>x_{\text{EtOH}}=0.171</math></b>			<b><math>x_{\text{EtOH}}=0.236</math></b>			<b><math>x_{\text{EtOH}}=0.319</math></b>		
<b>283</b>	1.38	1.18	<b>283</b>	1.14	1.09	<b>283</b>	0.82	0.93
<b>293</b>	2.43	1.99	<b>293</b>	1.82	1.65	<b>293</b>	1.37	1.41
<b>303</b>	3.98	3.25	<b>303</b>	2.95	2.45	<b>303</b>	2.00	1.98
<b>313</b>	6.33	5.18	<b>313</b>	4.60	3.79	<b>313</b>	3.29	2.79
<b>323</b>	9.64	7.85	<b>323</b>	6.96	5.43	<b>323</b>	4.64	3.98
<b>333</b>	14.29	11.74	<b>333</b>	10.32	7.80	<b>333</b>	6.52	5.62
<b>343</b>	21.32	17.62	<b>343</b>	15.07	11.76	<b>343</b>	9.57	7.94
<b>Pure EtOH</b>								
<b>283</b>	0.28	0.11						
<b>293</b>	0.44	0.17						
<b>303</b>	1.12	0.21						

313	2.43	0.33
323	3.68	0.38

214



215

216

217

218

219

220

221

### 3.2.Solubility correlation

222

#### 3.2.1. Van't Hoff empirical correlation

223

In order to confirm the results obtained, the solubility data of both polymorphs at different

224

temperatures is correlated by the Van't Hoff equation.

225

The Van't Hoff equation is the representation of the neperien logarithm of the molar fraction

226

solubility  $x_i$  of each polymorph as a function of the reciprocal absolute temperature for each

227

composition studied (cf. Fig.6). It is a simplification of the rigorous thermodynamics equation

228

given below [10] :

$$\ln(x_i \gamma_i) = -\frac{\Delta H_f}{RT} \left[ 1 - \frac{T}{T_f} \right] - \frac{1}{RT} \int_{T_f}^T \Delta C_p \, dT + \frac{1}{R} \int_{T_f}^T \frac{\Delta C_p}{T} \, dT \quad (3)$$

Where  $x_i$  is the molar fraction (-) of L-Glutamic acid polymorph  $i$  (i.e.  $\alpha$  or  $\beta$ ) in the solution at equilibrium,  $\gamma_i$  is the activity coefficient in the solution at equilibrium (-),  $T$  is the absolute temperature (K),  $\Delta H_f$  and  $T_f$  are, respectively, the enthalpy ( $\text{kJ}\cdot\text{mol}^{-1}$ ) and the temperature of fusion (K) of the considered polymorph,  $R$  is the ideal gas constant ( $\text{J}\cdot\text{mol}^{-1}\cdot\text{K}^{-1}$ ) and  $\Delta C_p$  is the difference between the heat capacity of the considered polymorph in the molten and the solid state ( $\text{J}\cdot\text{mol}^{-1}\cdot\text{K}^{-1}$ ). In the equation (3), the first term on the right side is more important than the other two terms containing  $\Delta C_p$ , which are often negligible and leads to the following equation (assuming  $\Delta C_p \approx 0$ ) [2,10] :

$$\ln(x_i \gamma_i) = -\frac{\Delta H_f}{RT} \left[ 1 - \frac{T}{T_f} \right] = -\frac{\Delta H_f}{RT} + \frac{\Delta S_f}{R} \quad (4)$$

The activity coefficient  $\gamma_i$  is linked to the excess Gibbs free energy. Since the Gibbs free energy of dissolution is the sum of the excess Gibbs free energy and of the Gibbs free energy of fusion, equation (4) can then be rewritten by introducing the enthalpy and the entropy of dissolution  $\Delta H_d$  and  $\Delta S_d$ , respectively. This leads to a reasonable simplification of equation (3) which is commonly used [2] :

$$\ln x_i = -\frac{\Delta H_d}{RT} + \frac{\Delta S_d}{R} \quad (5)$$

Fig.6 shows the Van't Hoff plots obtained for this work. It has to be noted that the curves present a good linearity and have the same trend for each solvent mixture. From the slope and the intercept point of the resulting straight lines, the enthalpy and the entropy of dissolution of both polymorphs in each water/ethanol solutions are determined. The results are reported in Table 2. Assuming that the slopes have the physical significance indicated by equation (5) (i.e.  $-\Delta H_d$ ), the difference in slopes reflects the differences in heats of dissolution of both polymorphs of L-Glutamic acid according to the ethanol molar fraction.

252 As presented in Table 2, the enthalpy and the entropy of dissolution of both polymorphs  
 253 increase with the increase of the ethanol molar fraction in the solvent mixture until a maximum  
 254 value (at  $x_{\text{EtOH}}=0.171$ ) then it tends to decrease significantly. Moreover,  $\beta$ -form exhibits a  
 255 higher dissolution enthalpy in water than  $\alpha$ -form but starting from a water/ethanol composition  
 256  $x_{\text{EtOH}}$  of 0.171, there is an inverse trend.

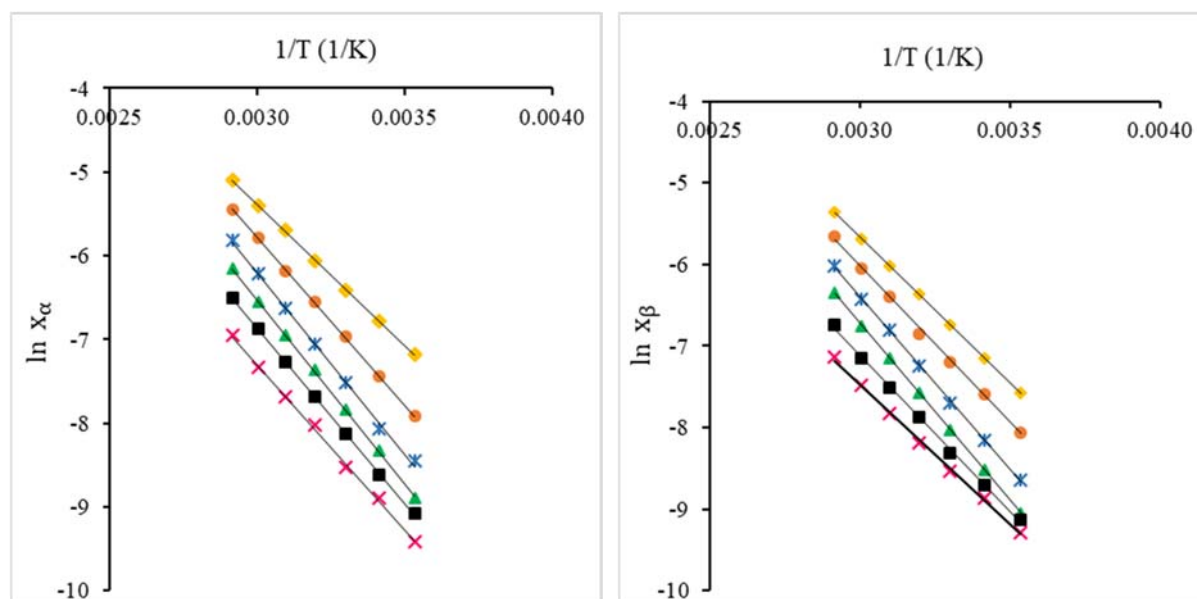
257 **Table 2**

258 Dissolution enthalpy and entropy of  $\alpha$  and  $\beta$  forms of L-Glutamic acid in different  
 259 water/ethanol mixtures.

	$\alpha$ -form			$\beta$ -form		
$x_{\text{EtOH}}$	$\Delta H_d$ (kJ.mol <sup>-1</sup> )	$\Delta S_d$ (kJ.mol <sup>-1</sup> K <sup>-1</sup> )	R <sup>2</sup>	$\Delta H_d$ (kJ.mol <sup>-1</sup> )	$\Delta S_d$ (kJ.mol <sup>-1</sup> K <sup>-1</sup> )	R <sup>2</sup>
<b>0</b>	27.96	39.03	0.9997	29.66	41.82	0.9999
<b>0.051</b>	33.30	51.85	0.9998	31.92	45.66	0.9982
<b>0.116</b>	35.99	56.38	0.9981	35.27	52.59	0.9997
<b>0.171</b>	35.51	55.29	0.9998	36.24	52.81	0.9999
<b>0.236</b>	34.86	47.51	0.9998	31.82	36.21	0.9983
<b>0.319</b>	32.73	37.52	0.9990	28.54	23.47	0.9983

260

261



262



263 **Fig. 6.** Van't Hoff plot for  $\alpha$  and  $\beta$  forms in ( $\blacklozenge$ ) pure water; ( $\bullet$ )  $x_{\text{EtOH}} = 0.051$ ;  
 264 ( $*$ )  $x_{\text{EtOH}} = 0.116$ ; ( $\blacktriangle$ )  $x_{\text{EtOH}} = 0.171$ ; ( $\blacksquare$ )  $x_{\text{EtOH}} = 0.236$ ; ( $\times$ )  $x_{\text{EtOH}} = 0.319$ .

265

### 266 3.2.2. Thermodynamic modeling

267 The solubility data in water/ethanol mixtures are also described by the Combined Nearly Ideal  
 268 Binary Solvent CNIBS/Redlich-Kister model suggested by Acree [19] and also used in different  
 269 studies [12,20,21].

$$270 \ln x_i = x_w \ln(x_i)_w + x_{\text{EtOH}} \ln(x_i)_{\text{EtOH}} + x_w x_{\text{EtOH}} \sum_{k=0}^N F_k (x_w - x_{\text{EtOH}})^k \quad (6)$$

271 Where  $x_w$  and  $x_{\text{EtOH}}$  refer in equation (6) to the initial molar fraction (-) respectively of water  
 272 and ethanol determined in the absence of L-Glutamic acid polymorph  $i$  ( $\alpha$  or  $\beta$ ),  $(x_i)_j$  is the  
 273 molar fraction solubility of the solute  $i$ , i.e. L-Glutamic acid polymorph, in pure solvent  $j$  (-),  
 274  $F_k$  are the parameters of the model; they relate the solute-solvent and solvent-solvent interaction  
 275 terms and are computed using a no-intercept least-squares analysis for each binary solvent  
 276 system (-) [21] and  $N$  is a number ranging from 0 to 3 for a ternary system (-).

277 Equation (6) describes how the solubility of a crystalline solute dissolved in a binary solvent  
 278 mixture evolves as a function of the composition of the medium at a fixed temperature.

279 By substituting  $x_w$  by  $(1 - x_{\text{EtOH}})$  in equation (6), for  $N=2$  [21] and with a subsequent  
 280 rearrangement and simplification, it leads to equation (7):

$$281 \ln x_i = \ln(x_i)_w + [\ln(x_i)_{\text{EtOH}} - \ln(x_i)_w + F_0 + F_1 + F_2] x_{\text{EtOH}} + [-F_0 - 3F_1 -$$

$$282 5F_2] x_{\text{EtOH}}^2 + [2F_1 + 8F_2] x_{\text{EtOH}}^3 + [-4F_2] x_{\text{EtOH}}^4 \quad (7)$$

283 To solve the equation, the solubility of the  $\beta$ -form in pure ethanol is measured by the  
 284 gravimetric method described above while the solubility values of the  $\alpha$ -form are taken from  
 285 the study of Long et al. [10].

286 The values of the parameters  $F_0$ ,  $F_1$  et  $F_2$  of equation (7) are listed in Table 3 together with the  
 287 root-mean square deviation (rmsd) defined by equation (8):

$$288 \text{ rmsd} = \left[ \frac{1}{n} \sum_{i=1}^n (x_i^{\text{cal}} - x_i^{\text{exp}})^2 \right]^{\frac{1}{2}} \quad (8)$$

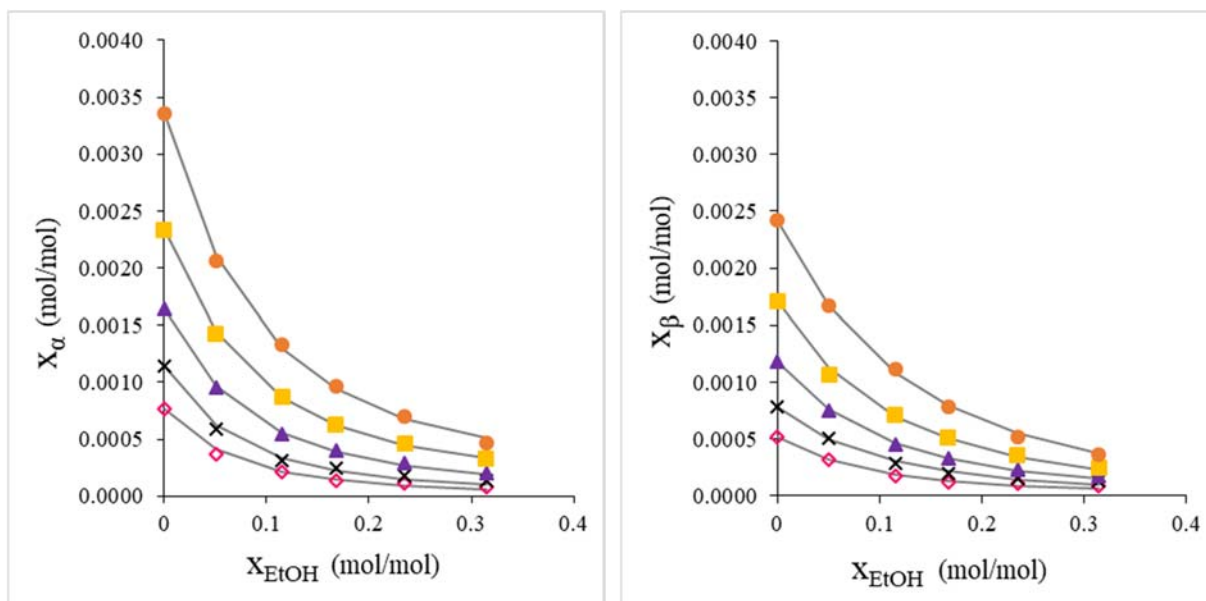
289 Where  $n$  is the number of experimental points,  $x_i^{\text{cal}}$  is the polymorph solubility calculated from  
 290 equation (7) and  $x_i^{\text{exp}}$  is the experimental polymorph solubility. Both are expressed here in  
 291 mol/mol.

292 The numerical results are presented in Fig.7 together with the experimental data taken from  
 293 Table 3. As expected, at constant temperature, the solubility of both forms of L-Glutamic acid  
 294 decreases with the increase of ethanol molar fraction. The experimental results can be well  
 295 described with the correlation (7) using two different parameter sets of the two polymorphs.  
 296 Thus, the model applied with  $N=2$  and based on three parameters, is well adapted to take into  
 297 account the effect of the solvent composition on the solubility.

298 **Table 3**

299 Fitting parameters of equation (7) for  $\alpha$  and  $\beta$  forms in different water/ethanol mixtures.

T (K)	$\alpha$ -form				$\beta$ -form			
	$F_0$	$F_1$	$F_2$	$10^5 \text{rmsd}$	$F_0$	$F_1$	$F_2$	$10^5 \text{rmsd}$
<b>283</b>	-5.400	-3.020	-1.689	2.55	-3.536	-1.908	-0.970	1.49
<b>293</b>	-5.209	-2.891	-1.596	3.18	-3.185	-1.661	-0.790	1.65
<b>303</b>	-4.870	-2.551	-1.298	1.68	-2.997	-1.548	-0.720	1.41
<b>313</b>	-4.674	-2.357	-1.130	1.05	-2.827	-1.427	-0.635	2.84
<b>323</b>	-4.502	-2.237	-1.044	3.45	-2.206	-1.017	-0.347	2.13



301

302 **Fig. 7.** Molar fraction solubility of  $\alpha$ -form and  $\beta$ -form in binary water/ethanol mixtures at  
 303 (●)  $T=323\text{K}$ ; (■)  $T=313\text{K}$ ; (▲)  $T=303\text{K}$ ; (×)  $T=293\text{K}$ ; (◇)  $T=283\text{K}$ ; (—) calculated  
 304 from equation (7).

305

#### 306 4. Conclusion

307 In this work, the solubility of both polymorphs of L-Glutamic acid in different water/ethanol  
 308 mixtures at temperature ranging between 283K and 343K are measured by a gravimetric  
 309 method. The results show that the solubility of the stable  $\beta$ -form is lower than the metastable  
 310  $\alpha$ -form regardless of the medium studied (water or water/ethanol mixtures). The results also  
 311 highlight that the solubility of both forms decreases with the increase of the antisolvent  
 312 concentration and increases with the temperature rising. The dissolution enthalpy and entropy  
 313 are also estimated by correlating the solubility measurements and the temperature using the  
 314 Van't Hoff equation. The measured solubility data are modeled by the CNIBS/Redlich  
 315 equation. Three parameters linked to the binary and ternary interactions between the three  
 316 species (solute, antisolvent and solvent) are determined using a no-intercept least-squares  
 317 analysis for each binary solvent system. This model gave a satisfactory correlation for a binary  
 318 mixture with optimized parameters.

319 Finally, the investigation of L-Glutamic acid's solubility in this work is prominent to the study  
320 of reverse antisolvent crystallization method and may also provide an indication for the  
321 screening of the solvent system in industry.

322

### 323 **List of symbol**

324	x	molar fraction ( $\text{mol}\cdot\text{mol}^{-1}$ )
325	m	mass (g)
326	M	molecular weight ( $\text{g}\cdot\text{mol}^{-1}$ )
327	$\Delta H_d$	enthalpy of dissolution ( $\text{kJ}\cdot\text{mol}^{-1}$ )
328	$\Delta H_f$	enthalpy of fusion ( $\text{kJ}\cdot\text{mol}^{-1}$ )
329	$\Delta S_d$	entropy of dissolution ( $\text{kJ}\cdot\text{mol}^{-1}\cdot\text{K}^{-1}$ )
330	$\Delta S_f$	entropy of fusion ( $\text{kJ}\cdot\text{mol}^{-1}\cdot\text{K}^{-1}$ )
331	R	gas constant ( $\text{J}\cdot\text{mol}^{-1}\cdot\text{K}^{-1}$ )
332	T	temperature (K)
333	$\Delta C_p$	heat capacity ( $\text{J}\cdot\text{mol}^{-1}\cdot\text{K}^{-1}$ )

334

### 335 **List of indices**

336	i	polymorphic form $\alpha$ or $\beta$
337	$\alpha$	$\alpha$ polymorph of L-Glutamic acid
338	$\beta$	$\beta$ polymorph of L-Glutamic acid
339	EtOH	Ethanol
340	w	water

341

342 **Acknowledgments**

343 We would like to thank Ruben Vera for the X-ray diffraction measurements (Centre de  
344 Diffractométrie Henry Longchambon, Université Lyon 1, Villeurbanne - France) and Eloise  
345 Thomas for the SEM images (Centre Technologique des Microstructures, Université Lyon 1,  
346 Villeurbanne - France).

347

348 **References**

- 349 [1] S. Veessler, F. Puel, Crystallization of Pharmaceutical Crystals, in: Handbook of Crystal  
350 Growth, Elsevier, 2015: pp. 915–949. [https://doi.org/10.1016/B978-0-444-56369-](https://doi.org/10.1016/B978-0-444-56369-9.00021-6)  
351 [9.00021-6](https://doi.org/10.1016/B978-0-444-56369-9.00021-6).
- 352 [2] J.W. Mullin, Crystallization, 4th ed, Butterworth-Heinemann, Oxford ; Boston, 2001.
- 353 [3] H.G. Brittain, K.K. Arora, S.X.M. Boerrigter, S.R. Byrn, P.W. Cains, A.J. Florence, D.J.R.  
354 Grant, Polymorphism in pharmaceutical solids, 2nd ed, Informa Healthcare, New York,  
355 2009.
- 356 [4] Z. Liu, L. Zhong, P. Ying, Z. Feng, C. Li, Crystallization of metastable  $\beta$  glycine from gas  
357 phase via the sublimation of  $\alpha$  or  $\gamma$  form in vacuum, Biophysical Chemistry. 132 (2008)  
358 18–22. <https://doi.org/10.1016/j.bpc.2007.10.003>.
- 359 [5] D. Mangin, F. Puel, S. Veessler, Polymorphism in Processes of Crystallization in Solution:  
360 A Practical Review, Organic Process Research & Development. 13 (2009) 1241–1253.  
361 <https://doi.org/10.1021/op900168f>.
- 362 [6] J. Bauer, S. Spanton, R. Henry, J. Quick, W. Dziki, W. Porter, J. Morris, Ritonavir: An  
363 Extraordinary Example of Conformational Polymorphism, (2001) 8.
- 364 [7] K. Srinivasan, P. Dhanasekaran, Nucleation control and crystallization of l-glutamic acid  
365 polymorphs by swift cooling process and their characterization, Journal of Crystal  
366 Growth. 318 (2011) 1080–1084. <https://doi.org/10.1016/j.jcrysgr.2010.11.050>.
- 367 [8] E. Chabanon, D. Mangin, C. Charcosset, Membranes and crystallization processes: State  
368 of the art and prospects, Journal of Membrane Science. 509 (2016) 57–67.  
369 <https://doi.org/10.1016/j.memsci.2016.02.051>.
- 370 [9] N.S. Tavaré, Micromixing limits in an MSMPR crystallizer, Chemical Engineering &  
371 Technology. 12 (1989) 1–11. <https://doi.org/10.1002/ceat.270120102>.
- 372 [10] B. Long, J. Li, Y. Song, J. Du, Temperature Dependent Solubility of  $\alpha$ -Form L -Glutamic  
373 Acid in Selected Organic Solvents: Measurements and Thermodynamic Modeling,  
374 Industrial & Engineering Chemistry Research. 50 (2011) 8354–8360.  
375 <https://doi.org/10.1021/ie200351b>.
- 376 [11] Y. Tahri, E. Gagnière, E. Chabanon, T. Bounahmidi, D. Mangin, Investigation of the l-  
377 Glutamic acid polymorphism: Comparison between stirred and stagnant conditions,  
378 Journal of Crystal Growth. 435 (2016) 98–104.  
379 <https://doi.org/10.1016/j.jcrysgr.2015.11.019>.
- 380 [12] Y. Mo, L. Dang, H. Wei, Solubility of  $\alpha$ -form and  $\beta$ -form of l-glutamic acid in different  
381 aqueous solvent mixtures, Fluid Phase Equilibria. 300 (2011) 105–109.  
382 <https://doi.org/10.1016/j.fluid.2010.10.020>.

- 383 [13] E. Manzurola, A. Apelblat, Solubilities of l-glutamic acid, 3-nitrobenzoic acid, p-toluic  
384 acid, calcium-l-lactate, calcium gluconate, magnesium-dl-aspartate, and magnesium-l-  
385 lactate in water, *The Journal of Chemical Thermodynamics*. 34 (2002) 1127–1136.  
386 <https://doi.org/10.1006/jcht.2002.0975>.
- 387 [14] H. Shi, F. Li, X. Huang, T. Wang, Y. Bao, Q. Yin, C. Xie, H. Hao, Screening and  
388 Manipulation of l-Glutamic Acid Polymorphs by Antisolvent Crystallization in an Easy-  
389 to-Use Microfluidic Device, *Ind. Eng. Chem. Res.* 59 (2020) 6102–6111.  
390 <https://doi.org/10.1021/acs.iecr.9b06566>.
- 391 [15] A. Shalmashi, A. Eliassi, Solubility of Salicylic Acid in Water, Ethanol, Carbon  
392 Tetrachloride, Ethyl Acetate, and Xylene, *Journal of Chemical & Engineering Data*. 53  
393 (2008) 199–200. <https://doi.org/10.1021/jc7004962>.
- 394 [16] M. Kitamura, Polymorphism in the crystallization of L-glutamic acid, *Journal of Crystal  
395 Growth*. 96 (1989) 541–546. [https://doi.org/10.1016/0022-0248\(89\)90049-3](https://doi.org/10.1016/0022-0248(89)90049-3).
- 396 [17] J. Cornel, C. Lindenberg, M. Mazzotti, Experimental Characterization and Population  
397 Balance Modeling of the Polymorph Transformation of l-Glutamic Acid, *Crystal Growth  
398 & Design*. 9 (2009) 243–252. <https://doi.org/10.1021/cg800387a>.
- 399 [18] J. Schöll, D. Bonalumi, L. Vicum, M. Mazzotti, M. Müller, In Situ Monitoring and  
400 Modeling of the Solvent-Mediated Polymorphic Transformation of L -Glutamic Acid,  
401 *Crystal Growth & Design*. 6 (2006) 881–891. <https://doi.org/10.1021/cg0503402>.
- 402 [19] W.E. Acree, Mathematical representation of thermodynamic properties Part 2. Derivation  
403 of the combined nearly ideal binary solvent (NIBS)/Redlich-Kister mathematical  
404 representation from a two-body and three-body interactional mixing model,  
405 *Thermochimica Acta*. 198 (1992) 71–79.
- 406 [20] Q. Chen, Y. Wang, X. Wu, J. Wang, Solubility of 11 $\beta$ -Hydroxypregna-1,4,16-triene-3,20-  
407 dione in Different Solvents, *Journal of Chemical & Engineering Data*. 53 (2008) 1414–  
408 1416. <https://doi.org/10.1021/jc800174u>.
- 409 [21] A. Jouyban, H.-K. Chan, N.Y.K. Chew, M. Khoubnasabjafari, Jr. William Eugene Acree,  
410 Solubility Prediction of Paracetamol in Binary and Ternary Solvent Mixtures Using  
411 Jouyban–Acree Model, *Chemical and Pharmaceutical Bulletin*. 54 (2006) 428–431.  
412 <https://doi.org/10.1248/cpb.54.428>.
- 413